UC San Diego
UC San Diego Previously Published Works

Title

Feeding induces translocation of vacuolar proton ATPase and pendrin to the membrane of leopard shark (Triakis semifasciata) mitochondrion-rich gill cells

Permalink

Authors

Roa, Jinae N
Munévar, Christian L
Tresguerres, Martin

Publication Date

2014-08-01

DOI

10.1016/j.cbpa.2014.04.003

Peer reviewed

CrossMark

Feeding induces translocation of vacuolar proton ATPase and pendrin to the membrane of leopard shark (*Triakis semifasciata*) mitochondrion-rich gill cells

Jinae N. Roa, Christian L. Munévar, Martin Tresguerres *

Marine Biology Research Division, Scripps Institution of Oceanography, University of California San Diego, 9500 Gilman Drive, La Jolla, CA 93092-0202, USA

ARTICLE INFO

ABSTRACT

In this study we characterized mitochondrion-rich (MR) cells and regulation of acid/base (A/B) relevant ion-transporting proteins in leopard shark (*Triakis semifasciata*) gills. Immunohistochemistry revealed that leopard shark gills posses two separate cell populations that abundantly express either Na$^+$/K$^+$-ATPase (NKA) or V-H$^+$-ATPase (VHA), but not both ATPases together. Co-immunolocalization with mitochondrial Complex IV demonstrated, for the first time in shark gills, that both NKA- and VHA-rich cells are also MR cells, and that all MR cells are either NKA- or VHA-rich cells. Additionally we localized the anion exchanger pendrin to VHA-rich cells, but not NKA-rich cells. In starved sharks, VHA was localized throughout the cell cytoplasm and pendrin was present at the apical pole (but not in the membrane). However, in a significant number of gill cells from fed leopard sharks, VHA translocated to the basolateral membrane (as previously described in dogfish), and pendrin translocated to the apical membrane. Our results highlight the importance of translocation of ion-transporting proteins to the cell membrane as a regulatory mechanism for A/B regulation.

© 2014 Elsevier Inc. All rights reserved.

1. Introduction

The fish gill epithelium has specialized cells that transport H$^+$ and HCO$_3^-$ between the blood and the surrounding water thus maintaining blood acid/base (A/B) homeostasis. Unlike the gills of teleost fishes, which transport ions for both A/B balance and osmoregulation, the gills of marine elasmobranchs transport ions exclusively for A/B regulatory purposes. Moreover, elasmobranch gills are responsible for ~97% of A/B regulation, with the rectal gland and kidneys facilitating iono- and osmoregulation, respectively (Heisler, 1988). The functional specificity of the elasmobranch gill makes it an excellent model for the study of A/B regulation at the cellular and systemic levels without interference from other ion-transporting processes.

In Atlantic stingray (*Dasyatis sabina*) (Piermarini and Evans, 2001), dogfish shark (*Squalus acanthias*) (Tresguerres et al., 2005), and bull shark (*Carcharhinus leucas*) (Reilly et al., 2011), Na$^+$/K$^+$-ATPase (NKA) and V-H$^+$-ATPase (VHA) are abundantly expressed in distinct gill cell subpopulations: NKA- and VHA-rich cells,

respectively. NKA-rich cells express apical Na$^+$/H$^+$ exchangers 3 (NHE3) and are considered "acid-secreting, base absorbing and sodium absorbing" cells (Choe et al., 2005, 2007; Reilly et al., 2011), while VHA-rich cells co-express an anion exchanger homologous to human pendrin (SLC26A4) and are considered "base-secreting, acid and chloride absorbing" cells (Piermarini et al., 2002; Reilly et al., 2011). Because NKA- and VHA-rich cells are specialized for active ion transport, both are thought to also be mitochondrion-rich (MR) cells (reviewed in Evans et al., 2005). However, only NKA-rich cells have been confirmed to also be MR cells, based on dual staining with anti-NKA antibodies and toluidine blue to highlight cell morphology (Wilson et al., 2002). While VHA-rich cells are typically assumed to also be MR cells based on their shape and location within the gill filament, there is no direct evidence supporting this assumption. It is also unknown whether all MR cells are either NKA- or VHA-rich cells or if other MR cell subtypes exist.

Normally, NKA is present in the cell basolateral membrane and VHA is located in cytoplasmic vesicles of elasmobranch gill cells. However, during experimentally induced blood alkalosis, VHA translocates into the basolateral membrane of dogfish gill cells (Tresguerres et al., 2005). The mechanism involves extra- and intracellular carbonic anhydrases that transfer increased plasma [HCO$_3^-$] inside gill cells (Gilmour et al., 2007; Tresguerres et al., 2007), where it is sensed by HCO$_3^-$-sensitive soluble adenylyl cylcase to produce cAMP, which

---

Abbreviations: VHA, V-H$^+$-ATPase, vacuolar proton ATPase; NKA, Na$^+$/K$^+$-ATPase, sodium potassium ATPase; MR, mitochondrion-rich.

* Corresponding author.
E-mail address: mtresguerres@ucsd.edu (M. Tresguerres).

triggers VHA translocation (Tresguerres et al., 2010, 2014). Basolateral VHA absorbs H^+ into the blood and energizes HCO_3^- secretion to seawater, thus counteracting blood alkalosis. In dogfish, the VHA translocation is essential for compensating naturally occurring alkalosis such as during the post-feeding blood alkalosis (Tresguerres et al., 2007). As H^+ is secreted into the stomach to aid in food digestion, an equimolar amount of HCO_3^- is absorbed into the blood, thus causing metabolic alkalosis (Wood et al., 2005, 2009). Similar to dogfish infused with $NaHCO_3$, VHA in gills from fed dogfish translocates to the basolateral membrane in a timeframe that is consistent with absorption of H^+ into the blood and secretion of excess HCO_3^- into seawater (Tresguerres et al., 2007). Presumably, the VHA translocation helps shape the typical 'alkaline tide'. While the alkaline tide has only been studied in detail in dogfish, it likely also takes place in most other marine elasmobranchs. In particular, leopard sharks (Triakis semifasciata) increase H^+ secretion into the stomach after a meal (Papastamatiou and Lowe, 2004, 2005) and thus should also experience postprandial blood alkalosis.

Intracellular HCO_3^- in VHA-rich cells is presumably exchanged for seawater Cl^- via apical pendrin (slc26a4). However, while several studies have suggested an involvement of pendrin in chloride uptake in freshwater fish (Perry et al., 2009; Piermarini et al., 2002), pendrin function has not been studied in relation to A/B regulation in fish gills. Intriguingly, pendrin seems predominantly located on the apical pole, but not directly in the apical membrane of gill cells from Atlantic stingray (Piermarini et al., 2002) and bull sharks (Reilly et al., 2011) acclimated to seawater. This raises the possibility that pendrin, like VHA, is translocated to the cell membrane during alkalosis.

In this study, we used immunofluorescence to investigate MR cells in leopard shark gills. We immunolabeled leopard shark gills to determine: (1) if NKA- and VHA-rich cells are distinct subpopulations, (2) if both NKA- and VHA-rich cells are also MR cells, (3) if all MR cells are either NKA- or NKA-rich cells, (4) localization of the anion exchanger pendrin, and (5) if feeding results in translocation of ion-transporting proteins to the cell membrane.

2. Materials and methods

2.1. Experimental animals

All experiments were approved by the SIO-UCSD animal care committee under protocol number #S10320 in compliance with the IACUC guidelines for the care and use of experimental animals. Juvenile leopard sharks were born in the experimental aquarium at Scripps Institution of Oceanography (SIO) from pregnant females caught from La Jolla Shores, CA, USA. Sharks were housed in tanks with flowing seawater and were fed chopped squid or mackerel 3 times a week. Samples were collected 2–3 days after feeding.

2.2. Feeding experiments

A total of 8 juvenile leopard sharks were used (mean body mass 145.5 ± 8.4 g; mean length 34.3 ± 0.83 cm; 3 male, 5 female), with 4 sharks in each treatment (starved vs. fed). Sharks were starved for five days, after which 4 randomly selected sharks were sacrificed and gill tissue collected ("starved" treatment). The remaining sharks were force-fed with blended squid worth ~5% of their body weight. After 24 h, sharks were sacrificed and gill tissue collected ("fed" treatment). The 24 h-post feeding sampling time was selected based on leopard shark gastric pH dynamics after feeding (Papastamatiou and Lowe, 2004), as well as systemic pH dynamics after feeding in dogfish sharks (Wood et al., 2005). Together with another study in dogfish (Tresguerres et al., 2007), the literature indicates that branchial base secretion in sharks is maximal or near maximal around 24 h after feeding.

2.3. Tissue preparation

Specimens were euthanized by an overdose of tricaine methanesulfonate (0.5 g·L^{-1}). Gill samples were fixed in 0.2 M cacodylate buffer, 3.2% paraformaldehyde, 0.3% glutaraldehyde for 6 h, transferred to 50% ethanol for 6 h, and stored in 70% ethanol until further processing for immunohistochemistry as described in Tresguerres et al. (2005).

2.4. Antibodies

Two commercially available anti-NKA antibodies were used for this study: monoclonal mouse anti-NKA antibodies raised against the chicken α-subunit (Developmental Studies Hybridoma Bank, Iowa City, IA, USA) and polyclonal rabbit anti-NKA antibodies raised against the mammalian α-subunit (Santa Cruz Biotechnology, Dallas, TX, USA). The mouse monoclonal anti-OxPhos antibody (Invitrogen, Grand Island, NY, USA) is against a highly conserved epitope in mitochondrial Complex IV, subunit 1. Antibodies against pendrin were raised against amino acids 630–643 from mammalian SLC26A4; these antibodies are known to specifically recognize pendrin from diverse elasmobranchs (Piermarini et al., 2002; Reilly et al., 2011). Custom-made polyclonal rabbit antibodies were against a conserved peptide in the VHA B-subunit (AREEVPGRRGFPGY). Fluorescent secondary antibodies goat anti-mouse Alexa Fluor 568 and goat anti-rabbit Alexa Fluor 488 were obtained from Invitrogen (Grand Island, NY, USA).

2.5. Western blot analysis

Frozen gill samples were weighed, immersed in liquid nitrogen, pulverized in a porcelain grinder, combined 1:10 w/v with ice-cold buffer (280 mM NaCl, 6 mM KCl, 5 mM $NaHCO_3$, 3 mM $MgCl_2$, 0.5 mM $NaSO_4$, 1 mM Na_2HPO_4, 350 mM urea, 70 mM trimethylamine N-oxide, 5 mM glucose, 1:100 protease inhibitor cocktail, Sigma), and homogenized using a glass homogenizer for 30 s. The sample was centrifuged at 3000 g for 10 min (4 °C) and the supernatant removed as the "crude homogenate fraction". Protein concentration was determined in triplicate using the Bradford method (Bio-Rad, Hercules, CA, USA). 5–20 μg of total protein was separated on 7.5% polyacrylamide mini gel (60 V 15 min, 200 V 45 min) and transferred to a polyvinylidene difluoride (PVDF) membrane (Bio-Rad). After transfer, PVDF membranes were incubated in blocking buffer (tris buffered saline, 1% tween, 5% milk) at room temperature for 1 h and incubated in the primary antibody at 4 °C overnight (anti-VHA = 1:1000). PVDF membranes were washed $3\times$ and incubated in secondary antibody (1:10,000) at room temperature for 1 h. Bands were made visible through addition of ECL Prime Western Blotting Detection Reagent (GE Healthcare, Waukesha, WI, USA) and imaged and analyzed in a BioRad Universal III Hood using ImageQuant software (BioRad). PVDF membranes incubated in blocking buffer with anti-VHA antibodies and 10-fold excess blocking peptide served as control and did not show any bands.

2.6. Immunohistochemistry

Gills fixed and stored in 70% ethanol as described above were serially dehydrated in 95% ethanol (10 min), 100% ethanol (10 min), and xylene (3 × 10 min). Tissues were transferred from xylene to paraffin (55 °C) (3 × 30 min), after which paraffin blocks were left to solidify overnight. Sections were cut at 7 μm using a rotary microtome; three consecutive sections of each sample were placed on slides and left on a slide warmer (37 °C) overnight. Paraffin was removed in xylene (10 min × 3) and sections rehydrated in 100% ethanol (10 min), 95% ethanol (10 min), 70% ethanol (10 min), and PBS. Non-specific binding was reduced by incubating the sections in blocking buffer (PBS, 2% normal goat serum, 0.02% keyhole limpet hemocyanin, pH 7.8) for 1 h.

Sections were then incubated in the primary antibody overnight at 4 °C (dilutions: anti-NKA = 1:500; anti-VHA = 1:500; anti-OxPhos = 1:500; anti-pendrin = 1:20). Slides were washed 3× in PBS and sections incubated in the appropriate secondary antibody (1:500) at room temperature for 1 h; followed by incubation with the nuclear stain Hoechst 33342 (Invitrogen, Grand Island, NY, USA) (5 μg/mL) for 5 min. Slides were then washed 3× in PBS and sections were permanently mounted in Fluorogel with tris buffer (Electron Microscopy Sciences, Hatfield, PA, USA). Immunofluorescence was detected using an epifluorescence microscope (Zeiss AxioObserver Z1) connected to a metal halide lamp and appropriate filters. Some images were captured using structured illumination (Zeiss Apotome2). Digital images were adjusted, for brightness and contrast only, using Zeiss Axiovision software and Adobe Photoshop. Antigen retrieval was required for anti-pendrin, which involved incubating slides in heated (95 °C) citrate unmasking buffer (10 mM citric acid, 0.05% Tween20, pH 6.0) for 20 min following rehydration. For anti-VHA, control sections were incubated in blocking buffer with anti-VHA antibodies and 10-fold excess blocking peptide.

2.7. Dual immunolocalization of NKA and VHA

Mouse anti-NKA and rabbit (1:500) anti-VHA (1:500) antibodies were diluted together in blocking buffer and applied onto slides as described above. Goat anti-mouse Alexa-Fluor 568 (1:500) and goat anti-rabbit Alexa-Fluor 488 (1:500) were diluted together and used for the secondary antibody incubation. Controls used to eliminate the possibility of cross-reactivity between antibodies included incubation with both primary antibodies together with only one secondary antibody, incubation with one primary antibody and both secondary antibodies, and incubation with only secondary antibodies. Control sections only stained positive when the corresponding primary and secondary antibodies were combined and no cross-reactivity was observed.

2.8. Colocalization of mitochondria, NKA, and VHA

For double immunolabeling of NKA and OxPhos, or VHA and OxPhos, sections were incubated in a solution of rabbit anti-NKA or rabbit anti-VHA antibodies (1:500) combined with mouse anti-OxPhos antibody (1:500); secondary antibodies and controls were as described in the previous section.

Co-localization with all three antibodies was achieved over two days. Initially, NKA- and VHA-rich cells were labeled with respective primary rabbit antibodies. Following incubation overnight, sections were washed as described above, incubated in the secondary Alexa-Fluor 488 anti-rabbit antibodies (1 h, room temperature), and washed. Sections were then incubated with mouse anti-OxPhos antibodies overnight, and ultimately with Alexa-Fluor 568 anti-mouse antibodies. This procedure resulted in both NKA and VHA immunolabeled in green, and mitochondria immunolabeled in red.

2.9. Immunolocalization of pendrin to NKA- and VHA-rich cells

For immunolocalization of pendrin to NKA- or VHA-rich cells sections were first incubated in rabbit anti-pendrin. Following incubation overnight, sections were washed as described above, incubated in the appropriate secondary antibodies (1 h, room temperature), washed again and blocked. Sections were then incubated with either mouse anti-NKA or rabbit anti-VHA antibodies overnight, and completed as described above.

2.10. Quantification of VHA and pendrin translocation

For VHA and pendrin translocation analyses, the number of cells displaying cytoplasmic or distinct membrane immunostaining was counted (Tresguerres et al., 2006, 2010) (basolateral membrane for VHA, apical membrane for pendrin). For each of the 4 specimens from each treatment (starved, fed), 3 immunostained gill sections were analyzed and all cells with positive VHA (total number of cells analyzed = 1310; 614 starved group; 696 fed group) or pendrin (total number of cells analyzed = 1839; 771 starved group; 1068 fed group) staining were counted at 300× and 600× magnification. Cells with distinct signal in the basolateral (VHA) or apical (pendrin) membrane were considered as having "Membrane staining" for each protein. Cells without distinct membrane staining (cytoplasmic and intermediate staining, see Tresguerres et al., 2006, 2010) were grouped together as "Cytoplasmic staining" for each protein. Percentages of total cells with either membrane or cytoplasmic staining were transformed to the arcsine of the square root of the value before statistical analysis. To test for differences in localization between starved (n = 4) and fed (n = 4) groups, separate t-tests were conducted for VHA- and pendrin-positive cells. Data are given as mean ± SEM and statistical significance was set at $P < 0.05$.

3. Results

3.1. Dual immunolocalization of NKA and VHA

The custom rabbit polyclonal anti-VHA antibodies recognized a 55 kDa band on western blots and labeled cells along the interlamellar region of the gill filament, but did not in control blots and sections when the antibody was combined with the blocking peptide (Fig. 1). Immunoreactivity of NKA and VHA was present in separate cell populations in the gills of leopard sharks. The anti-NKA antibody resulted in distinct basolateral staining, and the anti-VHA antibody resulted in primarily cytoplasmic staining, with only a few cells (less than 1%) showing basolateral staining. Based on double labeling with anti-NKA and anti-VHA antibodies on the same gill sections, NKA- and VHA-rich cells are distinct cell types (Fig. 2).

3.2. Colocalization of NKA and VHA with mitochondria

Anti-OxPhos antibodies strongly labeled cells in interlamellar regions of leopard shark gills. MR cells were visible at short exposure time but at longer exposure times all cells displayed positive signal as expected since all cells contain mitochondria (Fig. 3A). Cells with strong Oxphos signal also had strong NKA or VHA signal, indicating both NKA- and VHA-rich cells are also MR cells (Fig. 3B, C). To determine if NKA- and VHA-rich cells are the only MR cell subtypes present in leopard shark gills, NKA, VHA (both in green), and OxPhos (in red) were immunolabeled on the same section. The results showed that all MR cells are either NKA- or VHA-rich cells (Fig. 4).

3.3. Immunolocalization of pendrin in VHA-rich cells

In starved sharks, pendrin immunoreactivity was present in the apical pole (but not in the apical membrane) of cells along the interlamellar region. Pendrin immunoreactivity was specific to VHA-rich cells (Fig. 5A), with colocalization of pendrin and VHA found near the apical pole of VHA-rich cells (Fig. 5B). Pendrin was not present in NKA-rich cells (Fig. 5C).

3.4. Translocation of VHA and pendrin in gills from fed sharks

In starved leopard sharks, VHA and pendrin immunoreactivity was almost exclusively present in the cytoplasm (Fig. 6A, B; Table 1). However, feeding induced translocation of VHA to the basolateral membrane and pendrin to the apical membrane in a fraction of MR cells (Fig. 6C, D; Table 1). Optical sectioning and z-stack reconstruction confirmed membrane localization of both VHA and pendrin after feeding (Fig. 7).
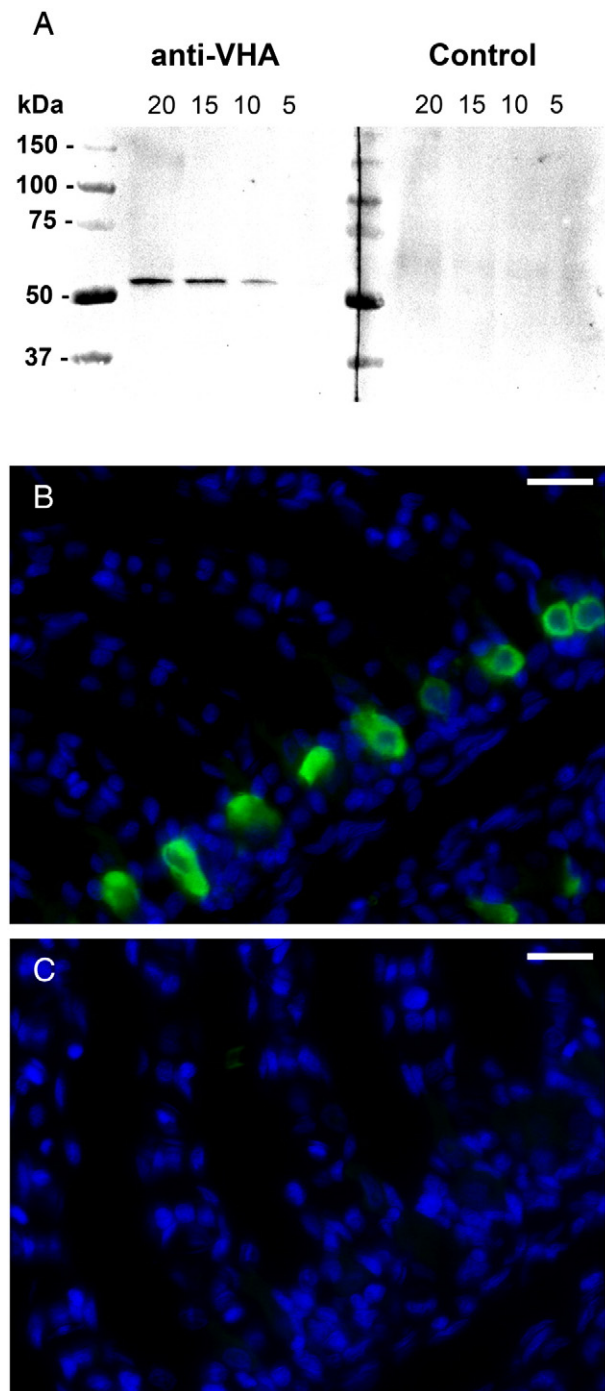
Fig. 1. Specificity of the anti-VHA antibodies in leopard shark gills. A) Western blot with gill crude homogenate showing a single and specific 55 kDa band when 20, 15, and 10 μg of total protein were loaded, but, at this exposure time, not in 5 μg (anti-VHA). The band was not evident when the antibodies were preincubated with excess blocking peptide (Control). B) VHA immunoreactivity in cells along the interlamellar region of a gill section. C) No signal was evident in the consecutive section treated anti-VHA antibodies preincubated with excess blocking peptide. VHA in green, nuclei in blue. Scale bar = 20 μm.

4. Discussion

Our results show that leopard shark gills have two distinct populations of NKA- and VHA-rich cells (likely acid- and base-secreting, respectively) (Evans et al., 2005; Tresguerres et al., 2005). We also established that both NKA- and VHA-rich cells are MR cells; to our knowledge this is the first time that this has been shown conclusively
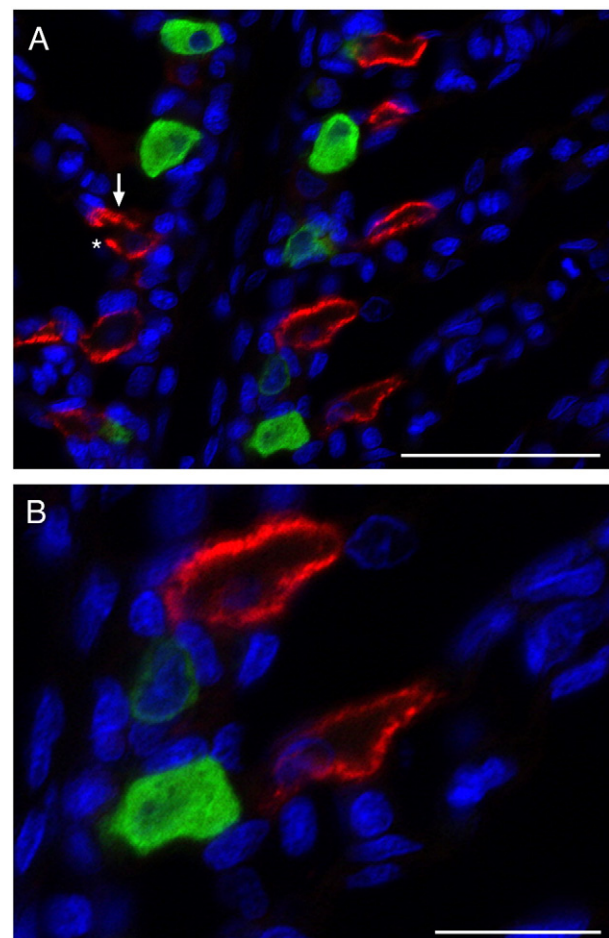

Fig. 2. NKA- and VHA-rich cells in leopard shark gills. Dual immunolocalization of NKA (red) and VHA (green), with NKA immunoreactivity along the basolateral membrane and VHA immunoreactivity diffuse throughout the cytoplasm. NKA- and VHA-rich cells were always observed as separate populations. An arrow and asterisk indicate basolateral and apical membranes on a representative cell, respectively. Nuclei in blue. Scale bar = 50 μm (A) or 20 μm (B).

for elasmobranch VHA-rich cells. Additionally, we showed that all MR cells in leopard shark gills are either NKA- or VHA-rich, suggesting all MR cells are either acid- or base-secreting. Further exploration revealed that pendrin is exclusively localized in VHA-rich cells. Lastly, feeding induced VHA translocation from cytoplasmic vesicles to the basolateral membrane and pendrin translocation to the apical membrane of a fraction of leopard shark gill cells.

4.1. NKA- and VHA-rich cells are MR cells

NKA immunoreactivity was always along the basolateral membrane and VHA immunoreactivity was generally distributed throughout the cytoplasm. NKA and VHA were expressed in separate cells, similar to Atlantic stingray (Piermarini et al., 2002; Piermarini and Evans, 2001), dogfish shark (Tresguerres et al., 2005), and bull shark (Reilly et al., 2011). The presence of NKA and VHA in two distinct cell populations separates elasmobranchs from teleost fishes. In freshwater teleosts, simultaneous expression of NKA and VHA is thought to drive Na$^+$ uptake and NH$_3$ excretion during osmoregulation and nitrogen balance (Evans, 2011), and has been shown in gills from rainbow trout (Galvez et al., 2002; Lin et al., 1994; Wilson et al., 2000a), killifish (Katoh et al., 2003), mudskipper (Wilson et al., 2000b), zebrafish (Liao et al., 2009), and several species of intertidal blennies (Uchiyama et al., 2012). Marine teleost gills also have several types of NKA-rich cells and although
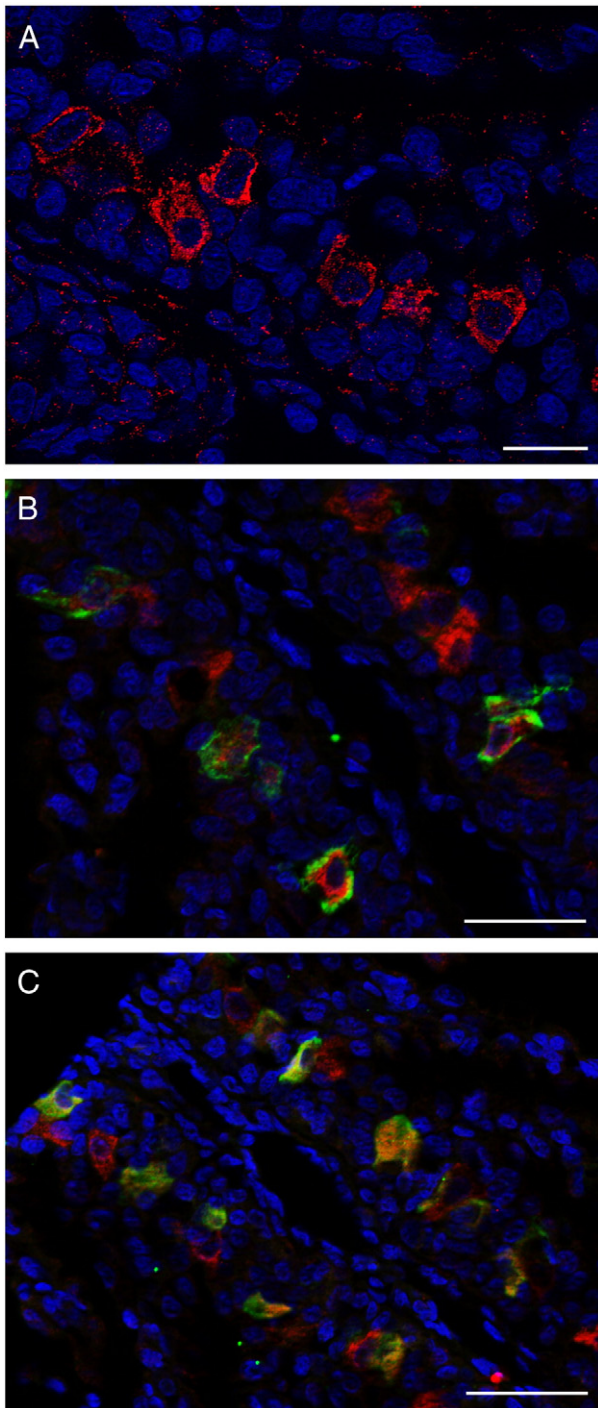
Fig. 3. NKA-, VHA-, and mitochondrion-rich (MR) cells in leopard shark gills. (A) MR cells, evident by strong anti-OxPhos immunoreactivity, were present along the interlamellar gill region. At longer exposure times all cells displayed a positive signal. Colocalization of NKA (B, green) or VHA (C, green) and MR cells (red) indicated that NKA- and VHA-rich cells are also MR cells. Nuclei in blue. Scale bar = 50 μm.

Fig. 4. Mitochondrion-rich (MR) cell types in leopard shark gills are enriched for NKA or VHA. Mitochondrial complex IV, indicative of MR cells (A, red) and NKA- and VHA-rich cells (B, both in green) were present throughout the interlamellar region. (C) MR cells were enriched in either NKA (distinct green signal along the basolateral membrane) or VHA (diffuse green signal throughout the cytoplasm, seen as yellow due to colocalization with mitochondrial complex IV (red). Nuclei in blue. Scale bar = 20 μm.

not widely reported, NKA and VHA may co-localize in the same cell as observed in a small population of branchial MR cells from longhorn sculpin (Catches et al., 2006). Thus, unlike teleost gill cells that carry out multiple ion-transporting functions and may express both pumps simultaneously, elasmobranch NKA- and VHA-rich cells are separate cell types specialized for A/B regulation.

To explore if NKA- and VHA-rich cells were also MR cells, we immunolabeled mitochondrial Complex IV (OxPhos) in leopard shark
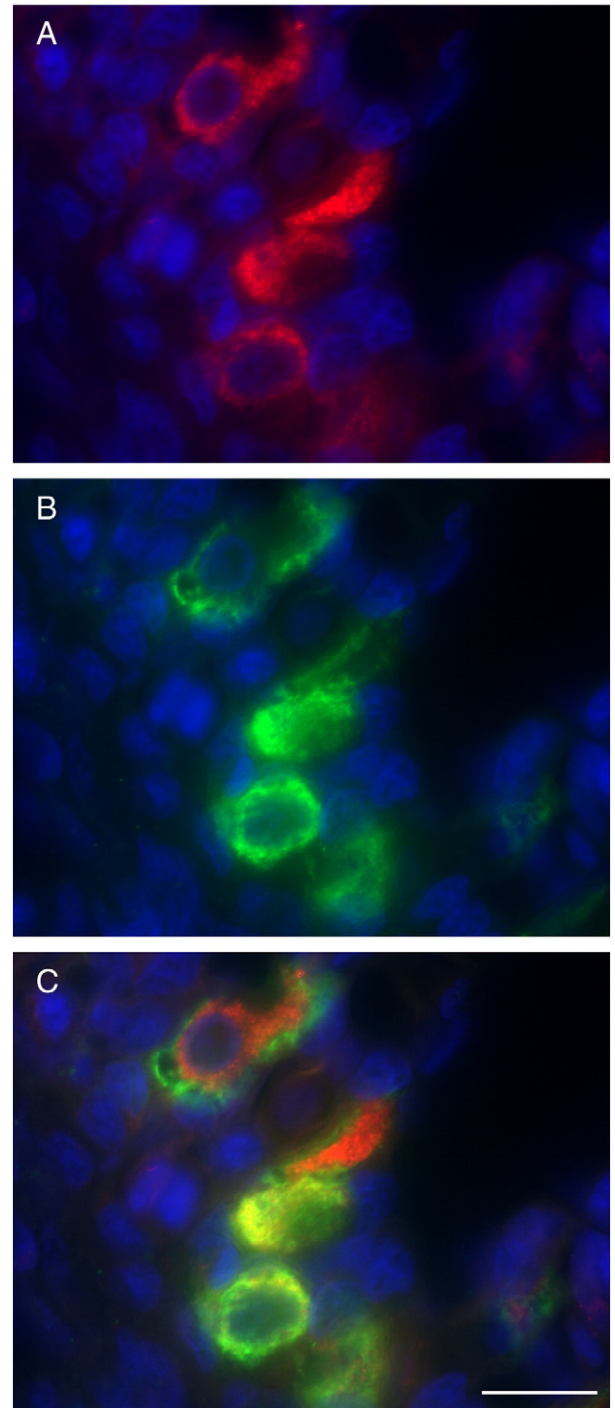
gills. Previously, MR cells were typically identified using qualitative structural analysis (Wilson et al., 1997, 2000b), vital dyes such as mitotracker (Galvez et al., 2002), or based on high NKA abundance (Edwards et al., 2002). Our results show it is possible to visualize MR cells by immunolabeling. Since Complex IV ("cytochrome c oxidase") is a highly conserved enzyme, these antibodies are useful in labeling MR cells from diverse species. In fact, our laboratory has successfully
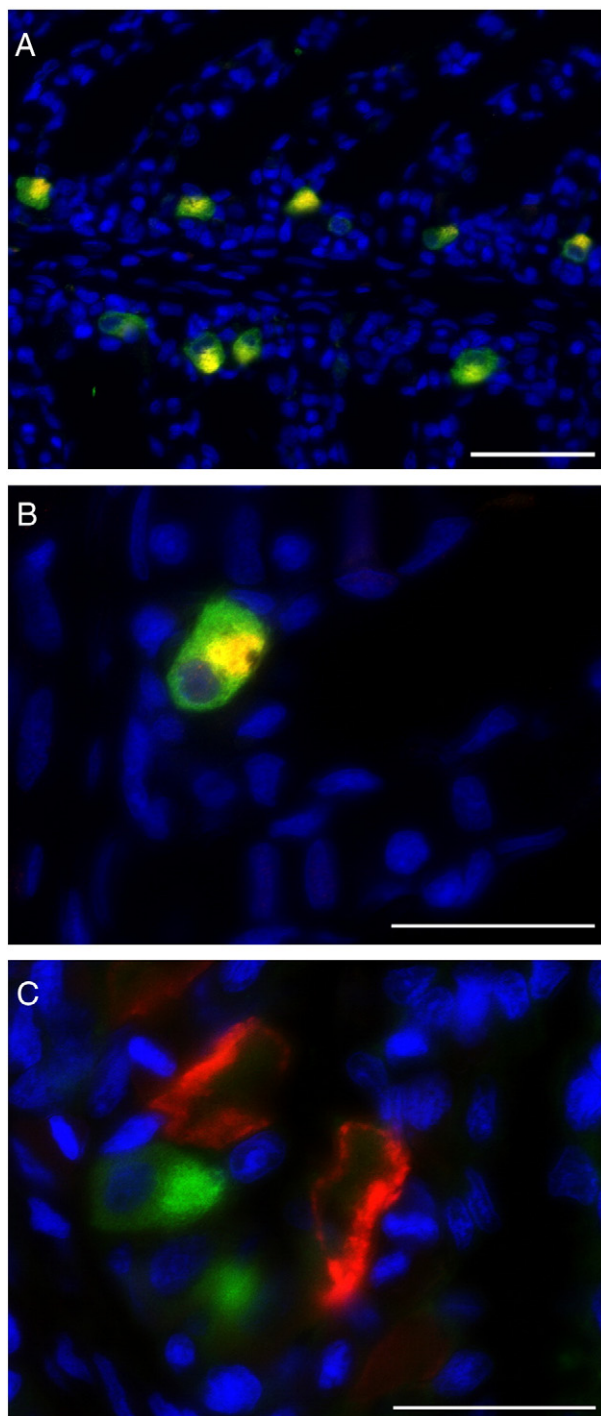
Fig. 5. Pendrin and VHA- or NKA-rich cells. A) Pendrin (red) and VHA (green) colocalization (yellow) was observed in gill cells along the interlamellar region. B) Pendrin immunoreactivity observed in the apical pole (but not in the membrane) of gill cells. C) Pendrin (green) and NKA (red) did not colocalize to the same cell. Nuclei in blue. Scale bar = 50 μm (A) or 20 μm (B, C).

used these antibodies in shark (this study), worm and coral tissues (unpublished observations). Although all cells have mitochondria, MR cells can be identified by intense OxPhos immunoreactivity at short exposure times. Numerous MR cells were observed along the interlamellar region of the gill; colocalization of OxPhos with NKA or VHA revealed that NKA- and VHA-rich cells were also MR cells. Additionally, prior to this study, the number of MR cell subtypes in elasmobranch gills was unknown; but we show here that there are two MR cell subtypes:

NKA- and VHA-rich cells. However, we cannot rule out the existence of MR, NKA- or VHA-rich, cell subtypes (*i.e.* cells that express either ATPase and differentially express other proteins).

Next, we investigated the relationship between NKA- and VHA-rich MR cells and another other ion-transporting protein, the anion exchanger pendrin. Pendrin immunoreactivity was present near the apical pole of a subset of gill cells and colocalized with VHA-rich cells (but not NKA-rich cells). These results support the hypothesis (Piermarini et al., 2002) that shark gill VHA-rich cells are functionally analogous to the mammalian base-secreting β-intercalated renal cells, which also express VHA and pendrin (Royaux et al., 2001). Since VHA-rich cells in shark gills are by far more abundant than in mammalian kidneys, they represent an excellent model for the study of cellular mechanisms for base secretion and further efforts should be pursued for developing cell cultures of these cells.

4.2. The effect of feeding on VHA and pendrin sub-cellular localization

Feeding induced translocation of VHA to the basolateral membrane, and of pendrin to the apical membrane in a fraction of gill cells from leopard sharks. Based on other established models for ion transport and A/B regulation such as dogfish (Tresguerres et al., 2005, 2006, 2007, 2010), bull shark (Reilly et al., 2011), and Atlantic stingray (Piermarini et al., 2002) gills, as well as mammalian kidney (Paunescu et al., 2008; Royaux et al., 2001), we expect that translocation of VHA and pendrin leads to upregulation of HCO_3^- secretion and H^+ absorption. In dogfish, feeding induces a pronounced blood alkalosis that is fully compensated ~24 h later ('alkaline tide') (Wood et al., 2005, 2009). Previous reports suggest that leopard sharks also undergo a post-feeding alkalosis (Papastamatiou and Lowe, 2004, 2005). Therefore, it is reasonable to assume that the translocation of VHA to the basolateral membrane and of pendrin to the apical membrane is a compensatory response to blood alkalosis.

The actual fraction of cells demonstrating VHA and pendrin translocation is likely proportional to the blood A/B stress. For example, distinct VHA translocation to the basolateral membrane occurred in 85% of VHA-positive gill cells from 12 h base-infused dogfish sharks, while it only occurred in 56% of VHA-positive cells in 6 h base-infused sharks (Tresguerres et al., 2006). Comparatively, sharks in our study demonstrated distinct VHA and pendrin translocation in ~10% of cells. This is likely explained by feeding inducing a much milder alkalosis compared to experimental base-infusion. We only quantified cells that had most VHA and pendrin in the cell membrane (distinct membrane staining) to conservatively consider cells that had became activated for HCO_3^- secretion. However, protein translocation is a dynamic and graded mechanism, and some of the cells that we categorized as "Cytoplasmic staining" likely had higher amounts of VHA and pendrin in their membranes compared to starved fish. Thus, our quantification method most likely underestimated the number of cells involved in base secretion.

To our knowledge, this is the first report of pendrin insertion into the apical membrane in response to alkalosis in an intact organism. However, cAMP-dependent translocation of pendrin to the apical membrane has previously been reported in rat cortical collecting duct (CCD) cells (Azroyan et al., 2012). Reports of VHA translocation to the cell membrane are more common, and they include translocation to the apical membrane in kidney (Gong et al., 2010; Paunescu et al., 2008), epididymis (Pastor-Soler et al., 2003), intestinal lumen (Collaco et al., 2013), blowfly salivary glands (Dames et al., 2006), and gills of the green shore crab (Weihrauch et al., 2002). In those organs, apical VHA secretes acid for diverse purposes such as blood A/B regulation, sperm inactivation, and ammonia excretion. In addition, VHA in sternal cells from the isopod *Pocellio scaber* is basolateral during $CaCO_3$ secretion and apical during $CaCO_3$ resorption (Ziegler et al., 2004). Translocation of VHA from the cytoplasm to the basolateral membrane has only been previously described in detail in dogfish gill cells (see Introduction); the
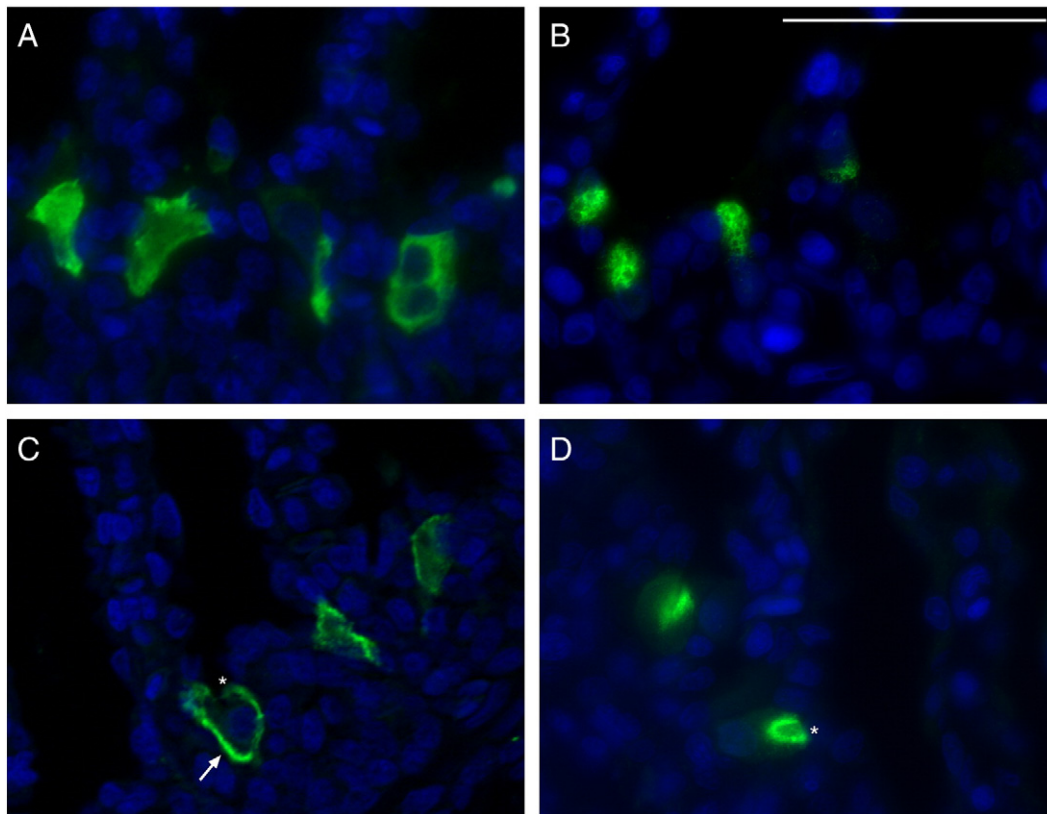
Fig. 6. VHA and pendrin immunoreactivity in the gills of starved and fed sharks. Representative images of cytoplasmic VHA (A) and pendrin (B) immunoreactivity in the gills of starved sharks. In fed sharks, VHA translocated to the basolateral membrane (C) and pendrin translocated to the apical membrane (D). An arrow and asterisks indicate basolateral and apical membranes on representative cells, respectively. VHA and pendrin in green, nuclei in blue. Scale bar = 20 μm.

current report suggests that it is a generalized mechanism to upregulate base secretion in elasmobranchs.

Importantly, translocation of pre-existing VHA protein, without the need for increased protein abundance, is enough to compensate for experimentally-induced, 6 h acute alkalosis (Tresguerres et al., 2006), as well as for dealing with post-feeding alkalosis (Tresguerres et al., 2007). For example, total VHA protein abundance did not change in gills from post-fed and 6 h base-infused dogfish sharks; but VHA protein abundance in the membrane increased significantly. Therefore, in the case of VHA and probably also pendrin, it is likely that protein translocation (not changes in gene expression) is more important during short term and physiological relevant changes in A/B status. Mechanisms such as protein translocation would not be evident using increasingly popular transcriptomic techniques such as qPCR or RNAseq, highlighting the importance of immunolocalization studies.

Table 1
Sub-cellular localization of VHA and pendrin in gills from starved and fed leopard sharks.

	Cytoplasmic (%)		Membrane (%)	
	Starved	Fed	Starved	Fed
VHA	99.49 ± 0.33	87.43 ± 0.73[*]	0.51 ± 0.33	12.57 ± 0.73[*]
Pendrin	99.83 ± 0.17	91.96 ± 2.51[*]	0.17 ± 0.17	8.04 ± 2.51[*]

Values for starved (n = 4) and fed (n = 4) sharks show percentage of cells demonstrating cytoplasmic, apical membrane (pendrin) or basolateral membrane (VHA) localization. Total number of cells analyzed, VHA = 1310 and pendrin = 1839.
　[*] Indicate a statistically significant difference compared to the respective starved group (t-test, see Materials and methods for details on data transformation).

5. Conclusions

In summary, our results showed that leopard shark gills, like all other elasmobranchs studied so far, have separate acid-secreting NKA-rich cells, and base-secreting VHA- and pendrin-rich cells. Our results also showed that these two cell types constitute all MR cells in the gill epithelium. However, we cannot discard the existence of further subtypes that differentially express other ion-transporting proteins or regulatory properties. The observed translocation of pendrin to the apical membrane in fed fish, together with the previously described VHA translocation to the basolateral membrane, indicates that translocation of multiple ion-transporting proteins to different regions within a cell is an important mechanism for the regulation of blood A/B status. This would be a dynamic and energetically efficient mechanism, and in some cases it may be more physiologically relevant compared to regulation of gene expression.
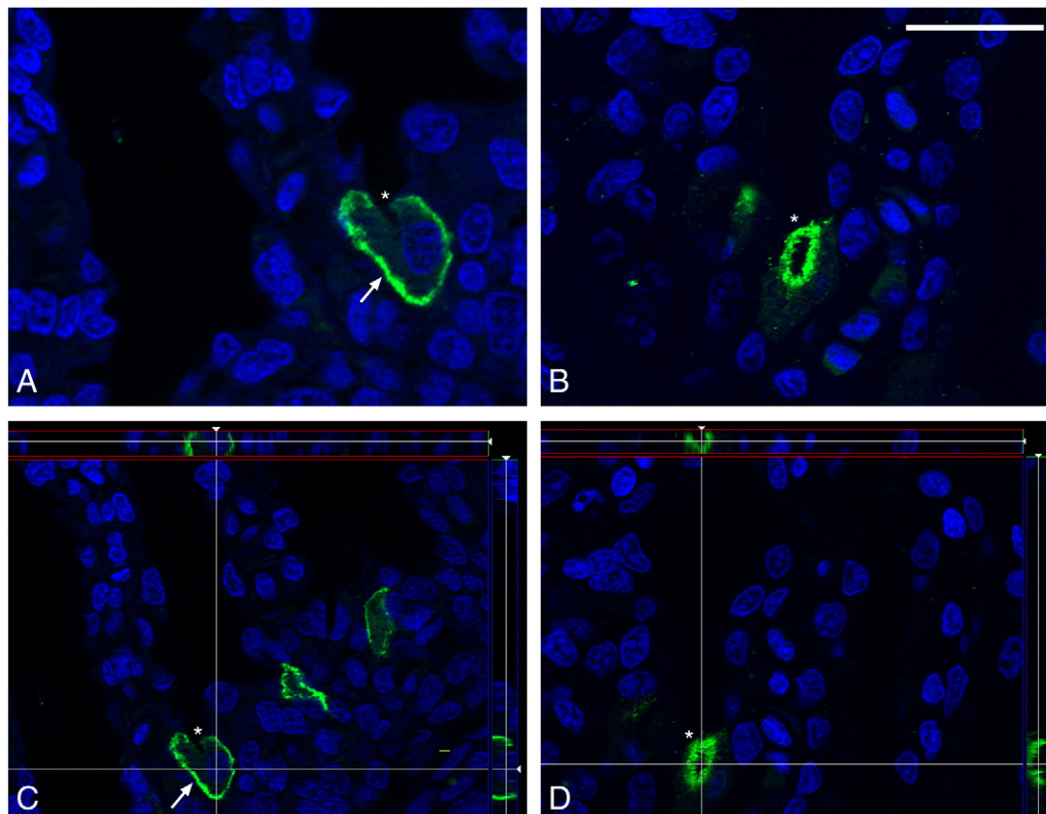
Fig. 7. Membrane localization of VHA and pendrin after feeding. Representative images of VHA in the basolateral membrane (A) and pendrin in the apical membrane (B) of branchial cells of fed leopard sharks. Images captured using optical sectioning and a Z-stack reconstruction of multiple images confined VHA (C) and pendrin (D) immunoreactivity to the membrane of its respective cell. Arrows and asterisks indicate basolateral and apical membranes on representative cells, respectively. VHA and pendrin in green, nuclei in blue. Scale bar = 20 μm.

References

Azroyan, A., Morla, L., Crambert, G., Laghmani, K., Ramakrishnan, S., Edwards, A., Doucet, A., 2012. Regulation of pendrin by cAMP: possible involvement in β-adrenergic-dependent NaCl retention. Am. J. Physiol. Ren. Physiol. 302, F1180–F1187.

Catches, J.S., Burns, J.M., Edwards, S.L., Claiborne, J.B., 2006. Na$^+$/H$^+$ antiporter, V-H$^+$-ATPase and Na$^+$/K$^+$-ATPase immunolocalization in a marine teleost (*Myoxocephalus octodecemspinosus*). J. Exp. Biol. 209, 3440–3447.

Choe, K.P., Kato, A., Hirose, S., Plata, C., Sindic, A., Romero, M.F., Claiborne, J.B., Evans, D.H., 2005. NHE3 in an ancestral vertebrate: primary sequence, distribution, localization, and function in gills. Am. J. Physiol. Regul. Integr. Comp. Physiol. 289, R1520–R1534.

Choe, K.P., Edwards, S.L., Claiborne, J.B., Evans, D.H., 2007. The putative mechanism of Na(+) absorption in euryhaline elasmobranchs exists in the gills of a stenohaline marine elasmobranch, *Squalus acanthias*. Comp. Biochem. Physiol. A Mol. Integr. Physiol. 146, 155–162.

Collaco, A.M., Geibel, P., Lee, B.S., Geibel, J.P., Ameen, N.A., 2013. Functional vacuolar ATPase (V-ATPase) proton pumps traffic to the enterocyte brush border membrane and require CFTR. Am. J. Physiol. Cell Physiol. 305, C981–C996.

Dames, P., Zimmermann, B., Schmidt, R., Rein, J., Voss, M., Schewe, B., Walz, B., Baumann, O., 2006. cAMP regulates plasma membrane vacuolar-type H$^+$-ATPase assembly and activity in blowfly salivary glands. Proc. Natl. Acad. Sci. U. S. A. 103, 3926–3931.

Edwards, S.L., Donald, J.A., Toop, T., Donowitz, M., Tse, C.-M., 2002. Immunolocalisation of sodium/proton exchanger-like proteins in the gills of elasmobranchs. Comp. Biochem. Physiol. A Mol. Integr. Physiol. 131, 257–265.

Evans, D.H., 2011. Freshwater fish gill ion transport: August Krogh to morpholinos and microprobes. Acta Physiol. (Oxf.) 202, 349–359.

Evans, D.H., Piermarini, P.M., Choe, K.P., 2005. The multifunctional fish gill: dominant site of gas exchange, osmoregulation, acid-base regulation, and excretion of nitrogenous waste. Physiol. Rev. 85, 97–177.

Galvez, F., Reid, S.D., Hawkings, G., Goss, G.G., 2002. Isolation and characterization of mitochondria-rich cell types from the gill of freshwater rainbow trout. Am. J. Physiol. Regul. Integr. Comp. Physiol. 282, R658–R668.

Gilmour, K.M., Bayaa, M., Kenney, L., McNeill, B., Perry, S.F., 2007. Type IV carbonic anhydrase is present in the gills of spiny dogfish (*Squalus acanthias*). Am. J. Physiol. Regul. Integr. Comp. Physiol. 292, R556–R567.

Gong, F., Alzamora, R., Smolak, C., Li, H., Naveed, S., Neumann, D., Hallows, K.R., Pastor-Soler, N.M., 2010. Vacuolar H$^+$-ATPase apical accumulation in kidney intercalated cells is regulated by PKA and AMP-activated protein kinase. Am. J. Physiol. Ren. Physiol. 298, F1162–F1169.

Heisler, N., 1988. Acid-base regulation. In: Shuttleworth, T.J. (Ed.), Physiology of Elasmobranch Fishes. Springer:Verlag, Berlin, pp. 215–252.

Katoh, F., Hyodo, S., Kaneko, T., 2003. Vacuolar-type proton pump in the basolateral plasma membrane energizes ion uptake in branchial mitochondria-rich cells of killifish *Fundulus heteroclitus*, adapted to a low ion environment. J. Exp. Biol. 206, 793–803.

Liao, B.-K., Chen, R.-D., Hwang, P.-P., 2009. Expression regulation of Na$^+$–K$^+$-ATPase alpha1-subunit subtypes in zebrafish gill ionocytes. Am. J. Physiol. Regul. Integr. Comp. Physiol. 296, R1897–R1906.

Lin, H., Pfeiffer, D., Vogl, A.W., Pan, J., Randall, D.J., 1994. Immunolocalization of H$^+$-ATPase in the gill epithelia of rainbow trout. J. Exp. Biol. 195, 169–183.

Papastamatiou, Y.P., Lowe, C.G., 2004. Postprandial response of gastric pH in leopard sharks (*Triakis semifasciata*) and its use to study foraging ecology. J. Exp. Biol. 207, 225–232.

Papastamatiou, Y.P., Lowe, C.G., 2005. Variations in gastric acid secretion during periods of fasting between two species of shark. Comp. Biochem. Physiol. A Mol. Integr. Physiol. 141, 210–214.

Pastor-Soler, N., Beaulieu, V., Litvin, T.N., Da Silva, N., Chen, Y., Brown, D., Buck, J., Levin, L.R., Breton, S., 2003. Bicarbonate-regulated adenylyl cyclase (sAC) is a sensor that regulates pH-dependent V-ATPase recycling. J. Biol. Chem. 278, 49523–49529.

Paunescu, T.G., Da Silva, N., Russo, L.M., McKee, M., Lu, H.A.J., Breton, S., Brown, D., 2008. Association of soluble adenylyl cyclase with the V-ATPase in renal epithelial cells. Am. J. Physiol. Ren. Physiol. 294, F130–F138.

Perry, S.F., Vulesevic, B., Grosell, M., Bayaa, M., 2009. Evidence that SLC26 anion transporters mediate branchial chloride uptake in adult zebrafish (*Danio rerio*). Am. J. Physiol. Regul. Integr. Comp. Physiol. 297, R988–R997.

Piermarini, P.M., Evans, D.H., 2001. Immunochemical analysis of the vacuolar proton-ATPase B-subunit in the gills of a euryhaline stingray (*Dasyatis sabina*): effects of salinity and relation to Na(+)/K(+)-ATPase. J. Exp. Biol. 204, 3251–3259.

Piermarini, P.M., Verlander, J.W., Royaux, I.E., Evans, D.H., 2002. Pendrin immunoreactivity in the gill epithelium of a euryhaline elasmobranch. Am. J. Physiol. Regul. Integr. Comp. Physiol. 283, R983–R992.

Reilly, B.D., Cramp, R.L., Wilson, J.M., Campbell, H.A., Franklin, C.E., 2011. Branchial osmoregulation in the euryhaline bull shark, *Carcharhinus leucas*: a molecular analysis of ion transporters. J. Exp. Biol. 214, 2883–2895.

Royaux, I.E., Wall, S.M., Karniski, L.P., Everett, L.A., Suzuki, K., Knepper, M.A., Green, E.D., 2001. Pendrin, encoded by the Pendred syndrome gene, resides in the apical region of renal intercalated cells and mediates bicarbonate secretion. Proc. Natl. Acad. Sci. U. S. A. 98, 4221–4226.

Tresguerres, M., Katoh, F., Fenton, H., Jasinska, E., Goss, G.G., 2005. Regulation of branchial V-H$^+$-ATPase, Na$^+$/K$^+$-ATPase and NHE2 in response to acid and base infusions in the Pacific spiny dogfish (*Squalus acanthias*). J. Exp. Biol. 208, 345–354.

Tresguerres, M., Parks, S.K., Katoh, F., Goss, G.G., 2006. Microtubule-dependent relocation of branchial V-H$^+$-ATPase to the basolateral membrane in the Pacific spiny dogfish (*Squalus acanthias*): a role in base secretion. J. Exp. Biol. 209, 599–609.

Tresguerres, M., Parks, S.K., Wood, C.M., Goss, G.G., 2007. V-H$^+$-ATPase translocation during blood alkalosis in dogfish gills: interaction with carbonic anhydrase and involvement in the postfeeding alkaline tide. Am. J. Physiol. Regul. Integr. Comp. Physiol. 292, R2012–R2019.

Tresguerres, M., Parks, S.K., Salazar, E., Levin, L.R., Goss, G.G., Buck, J., 2010. Bicarbonate-sensing soluble adenylyl cyclase is an essential sensor for acid/base homeostasis. Proc. Natl. Acad. Sci. U. S. A. 107, 442–447.

Tresguerres, M., Barott, K.L., Barron, M.E., Roa, J.N., 2014. Established and potential physiological roles of bicarbonate-sensing soluble adenylyl cyclase (sAC) in aquatic animals. J. Exp. Biol. 217, 663–672.

Uchiyama, M., Komiyama, M., Yoshizawa, H., 2012. Structures and immunolocalization of Na$^+$, K$^+$-ATPase, Na$^+$/H$^+$ exchanger 3 and vacuolar-type H$^+$-ATPase in the gills of blennies (Teleostei: Blenniidae) inhabiting rocky intertidal areas. J. Fish Biol. 80, 2236–2252.

Weihrauch, D., Ziegler, A., Siebers, D., Towle, D.W., 2002. Active ammonia excretion across the gills of the green shore crab *Carcinus maenas*: participation of Na$^+$/K$^+$-ATPase, V-type H$^+$-ATPase and functional microtubules. J. Exp. Biol. 205, 2765–2775.

Wilson, J.M., Randall, D.J., Vogl, A.W., Iwama, G.K., 1997. Immunolocalization of proton-ATPase in the gills of the elasmobranch, *Squalus acanthias*. J. Exp. Zool. 278, 78–86.

Wilson, J.M., Laurent, P., Tufts, B.L., Benos, D.J., Donowitz, M., Vogl, A.W., Randall, D.J., 2000a. NaCl uptake by the branchial epithelium in freshwater teleost fish: an immunological approach to ion-transport protein localization. J. Exp. Biol. 203, 2279–2296.

Wilson, J.M., Randall, D.J., Donowitz, M., Vogl, A.W., Ip, A.K., 2000b. Immunolocalization of ion-transport proteins to branchial epithelium mitochondria-rich cells in the mudskipper (*Periophthalmodon schlosseri*). J. Exp. Biol. 203, 2297–2310.

Wilson, J.M., Morgan, J.D., Vogl, A.W., Randall, D.J., 2002. Branchial mitochondria-rich cells in the dogfish *Squalus acanthias*. Comp. Biochem. Physiol. A Mol. Integr. Physiol. 132, 365–374.

Wood, C.M., Kajimura, M., Mommsen, T.P., Walsh, P.J., 2005. Alkaline tide and nitrogen conservation after feeding in an elasmobranch (*Squalus acanthias*). J. Exp. Biol. 208, 2693–2705.

Wood, C.M., Schultz, A.G., Munger, R.S., Walsh, P.J., 2009. Using omeprazole to link the components of the post-prandial alkaline tide in the spiny dogfish, *Squalus acanthias*. J. Exp. Biol. 212, 684–692.

Ziegler, A., Weihrauch, D., Hagedorn, M., Towle, D.W., Bleher, R., 2004. Expression and polarity reversal of V-type H$^+$-ATPase during the mineralization-demineralization cycle in *Porcellio scaber* sternal epithelial cells. J. Exp. Biol. 207, 1749–1756.